Evidence for low-level jets caused by coastal baroclinity at the Kurzeme shore of the Baltic Sea

Tija Sīle, Juris Seņņikovs and Uldis Bethers

Laboratory for Mathematical Modelling of Environmental and Technological Processes, Department of Physics, University of Latvia, Zeļļu St. 23, LV-1002, Riga, Latvia; tija.sile@lu.lv

Abstract. Observational wind direction data from meteorological stations along the Kurzeme coast of the Baltic Sea were analysed for the years 1966–2015. The data show that during the daytime in the warm season the winds that aligned with the coastline (northern and southwestern) are more frequent than those from any other direction. A case study was carried out using the Weather Research and Forecast Numerical Weather Prediction model and Advanced Scatterometer wind data to investigate the mechanisms causing the increased frequency of northern winds. The results show a coast-parallel wind flow over the sea that extends for 50 km from the shore and several hundred metres above the sea level. It can be classified as a low-level jet – an air flow where the vertical wind speed distribution has a maximum in the lowest kilometre of the atmosphere. The flow is geostrophic and can be described using the thermal wind expression where wind shear is linked with temperature differences over the coast, therefore allowing classifying the event as a coastal low-level jet.

Key words: geostrophic wind, sea breeze, low-level jet, coastal low-level jet, Baltic Sea, Kurzeme.

INTRODUCTION

An accurate description of coastal wind climate is important for wind energy and port planning (Soomere & Keevallik 2001). Wind climate also influences the air quality of coastal cities (Miller et al. 2003). Sea breeze can have a significant impact on the temperature in the region (Lebassi et al. 2009). Precise operational forecasts of wind and sea conditions are necessary for search and rescue operations.

To investigate the climatological properties of wind, data from meteorological observation stations can be employed. They have long time series and good spatial coverage in most regions; however, the quality of data can be influenced by the siting of the station and nearby obstacles. High-precision measurements are made during specialized campaigns in the context of wind energy applications, but they are available only for a limited number of locations and time periods.

A comparatively recent trend is the application of remote sensing in meteorological measurements. In the case of wind, the data source is the sensors located on the meteorological satellites that can measure fields over water bodies, e.g., Advanced SCATterometer sensors (ASCAT) on the METOP A and B satellites (EUMETSAT). The instantaneous wind speed and direction are provided on a 12.5 km grid and each location is measured once or twice a day.

The values of the physical parameters of water bodies differ from those of land surface and in some cases this difference can create atmospheric flows on its own. The most popular example is the sea breeze, where due to the temperature differences a circulation forms in the lowest levels of the atmosphere. Although in the idealized case the flow is perpendicular to the coast, in realistic scenarios it can also be oriented at an angle to the coastline (Miller et al. 2003). In these cases, accounting for the influence of the larger-scale pressure distribution (prevailing geostrophic wind direction) leads to the distinction between corkscrew and backdoor breezes. In the Northern Hemisphere the convergence (divergence) caused by geostrophic wind with the coast to the left (right) hand strengthens (weakens) the sea breeze circulation and is called corkscrew (backdoor) sea breeze (Miller et al. 2003; Steele et al. 2015).

The term 'low-level jet' (LLJ) describes a state where the vertical distribution of the horizontal wind speed has a maximum in the lower kilometre of the atmosphere. There are several processes that create LLJs (Stensrud 1996) and two of them are directly relevant to coastal meteorology.

The first process is baroclinity, where thermal wind relationship describes the vertical wind shear caused by the horizontal temperature gradient (Lin 2007). Coastal low-level jets (CLLJs) are created by the temperature gradients between warmer land and colder sea surfaces. They have been observed in most continents (Ranjha et al. 2013). The structure of the jet can be influenced by orography and topography, for example, if the coastline has bays and capes, local acceleration caused by hydraulic effects has been reported downwind from the capes (Burk & Thompson 1996).

The second process is inertial oscillation, where the diurnal friction changes in the boundary layer lead to an LLJ after the sunset when the friction decreases (Lin 2007). A spatial analogue of the inertial oscillation has been invoked to explain the LLJ that is created when the warm air mass from the land is advected over the cooler water. The warm air advection can lead to stable atmospheric conditions or the development of internal boundary layers (Smedman et. al. 1993). Low-level jets are reported to be present over the Baltic Sea 40–45% of time during late spring (Svensson et al. 2016). Similarly, LLJs caused by various mechanisms can often be present in the Arctic region (Tuononen et al. 2015).

Using an idealized model, Tjernstrom & Grisogono (1996) reported a jet along the Swedish shore in the morning before the onset of sea breeze. They concluded that the jet was created by coastal topography with a possible additional role of baroclinity.

The term 'jet' can also refer to a wind maximum in the horizontal dimension. A similarly named but physically different coastal jet mechanism describes such a wind maximum parallel to the shoreline caused by roughness changes between water and dry land in the presence of temperature inversion (Hunt et al. 2004).

In this study the diurnal cycle of the observed wind direction in the Kurzeme coastal stations of the Baltic Proper is analysed. The results show an increased frequency of shore parallel winds, form the southwestern and northern directions. A case study is then carried out to investigate the physical mechanisms that could explain an increased frequency of northern winds. Modelling results indicate the presence of an LLJ.

DATA AND METHODS

The study area is located in the eastern part of the Baltic Sea (Fig. 1). The coastline from Liepaja to Kolka is relatively simple and there are no islands.

Two sets of 10 m wind observation data from the Latvian Environment, Geology and Meteorology Centre (LEGMC) were used in this study. The station locations are shown in Fig. 1. First, observations with a temporal resolution of 1 h or 3 h from the years 1966–2015 were used for climatological analysis. The time series were converted from local time to UTC. As there are three times more data points from hourly observations covering the same time interval than from the observations with 3 h intervals, the hourly observations were assigned one third of the weight in the calculations.

To describe the climatological diurnal cycle of wind direction, the day was divided into 3 h intervals (e.g. 02:00–04:00, 05:00–07:00). For each time interval the
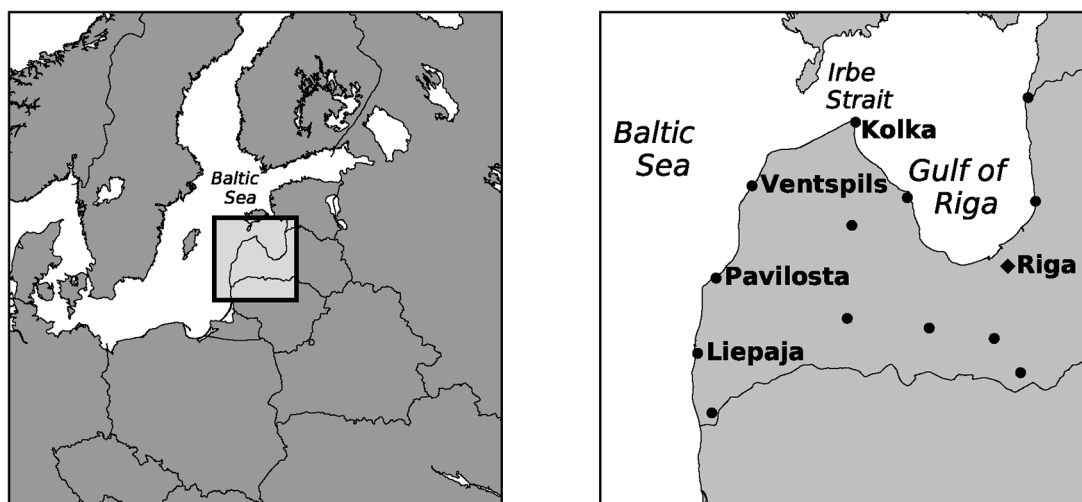

Fig. 1. Location of the study domain (left) and the locations of the LEGMC meteorological stations that carry out wind observations (right). The coastal stations of the Baltic Proper have their names displayed.

wind direction distribution, i.e., the probability P of the wind blowing from direction d was calculated as

$$P_d = \frac{n_d}{\sum_{i=1}^{16} n_i}, \qquad (1)$$

where n_i is the number of instances of the wind from the ith direction. Sixteen wind direction bins were used, i.e., S, SSE, SE, etc. The empirical distribution function P was calculated for each day of the year, where n was counted using data for the 11 nearest calendar days – 5 days before and 5 days after the day of the interest for the years 1966–2015.

Two additional observation data sets were used for the case study. The second data set of conventional meteorological observations contains time series with 1 min temporal resolution and was used after smoothing by calculating the 10 min running average. This data set has been available only since 2009 and only in selected meteorological stations.

The third observational data set comes from ASCAT, which is a remote sensing instrument used to measure wind fields over water bodies (Verhoef & Stoffelen 2013). For the case study two ASCAT products optimized for coastal zones on a 12.5 km grid were used (Metop-A and Metop-B Coastal Wind, available since 2010 and 2012, respectively). The availability of data depends on satellite trajectories and each measurement consists of two approximately 500 km wide swaths. They typically fly over the study region twice a day – between 11:00 and 14:00 (08:00 and 11:00 UTC) and between 20:00 and 23:00 (17:00 and 20:00 UTC). Here and further in the text local time is defined as UTC + 03 h corresponding to summer time.

The Weather Research and Forecast (WRF) model (version 3.6.1) was used for the case study. Three nested domains with a grid resolution of 27 km (250×199 points in the east–west and south–north directions, respectively), 9 km (352×280) and 3 km (400×400) and 91 vertical levels were used. The Kain–Fritsch cumulus parametrization (Kain 2004) was used for the two outer domains (no cumulus scheme for the innermost domain). The WRF Single Moment (WSM-5, Hong et al. 2004) scheme was used for the microphysics and the RRTM/Dudhia scheme was used for longwave/shortwave radiation parametrization (Dudhia 1989; Mlawer et al. 1997). The Yonsei University Scheme was used for Planetary Boundary Layer (PBL) parametrization (Hong et al. 2006). The ERA-Interim reanalysis dataset was used for initial and lateral boundary conditions (Dee et al. 2011). The NOAA/NCEP (National Oceanic and Atmospheric Administration / National Centers for Environmental Prediction) high-resolution Real Time

Global 1/12° Sea Surface Temperature dataset was used for the sea surface boundary conditions (Gemmill et al. 2007). The length of the model run was 48 h and it was initialized at 18:00 UTC on the previous day.

The choice of the PBL parametrization scheme for the modelling of LLJs using WRF was analysed by Nunalee & Basu (2014). They found that many PBL schemes show similar performance.

The initial analysis of model results showed that the calculation of the geostrophic wind could be useful. The geostrophic wind (u_g, v_g) is defined as the wind that would satisfy the balance between the Coriolis force and the horizontal gradient of pressure p. Several equivalent expressions are available for its calculation, using either spatial derivatives of pressure or of geopotential height. Both fields are provided by standard WRF output, although with vertical coordinate expressed in terms of the model levels (the eta-coordinate). The pressure field was linearly interpolated to constant heights at each grid point, and then the expressions

$$f u_g = -\frac{1}{\rho} \frac{\partial p}{\partial y}, \qquad (2)$$

$$f v_g = \frac{1}{\rho} \frac{\partial p}{\partial x}, \qquad (3)$$

were used to calculate the geostrophic wind components, where f is the Coriolis parameter, $f = 1.2 \times 10^{-4}\ \text{s}^{-1}$, and x and y are the horizontal coordinates, oriented in the east–west and north–south directions, respectively. The density field p was calculated from the pressure and temperature at each grid point. The geostrophic wind relationship is usually defined in the synoptic spatial scale (see, for instance, Holton 2004), therefore the pressure field was smoothed horizontally using a moving average filter and 15×15 km window (5 grid points in both directions). The smoothing procedure was carried out after the interpolation on constant height levels but before the calculation of spatial derivatives. In literature, smoothing over even larger windows has been used, e.g, Floors et al. (2015) averaged over a 300 km window. Previous studies have typically used larger model grid sizes, e.g., 45 km in Muñoz & Garreaud (2005).

RESULTS

Climatological analysis of the meteorological station data

The long-term observational wind direction data in coastal meteorological stations can be used to estimate the climatic wind direction distribution and its diurnal

cycle. Figure 2 shows the equivalent of a traditional wind rose with another axis added representing the time of the day. The wind directions are on the *x*-axis and the time of day (local time) is on the *y*-axis. Results for the Ventspils station (see Fig. 1 for location) for a late spring day (15 May, Fig. 2A) show that the wind direction distribution is heterogeneous and has a pronounced diurnal cycle. Two directions occur between sunrise and sunset (indicated by horizontal black lines) which are more frequent than the others – southwestern and northern wind. For the Ventspils observation station these directions are approximately parallel to the coastline (indicated by vertical black lines in Fig. 2A, see also
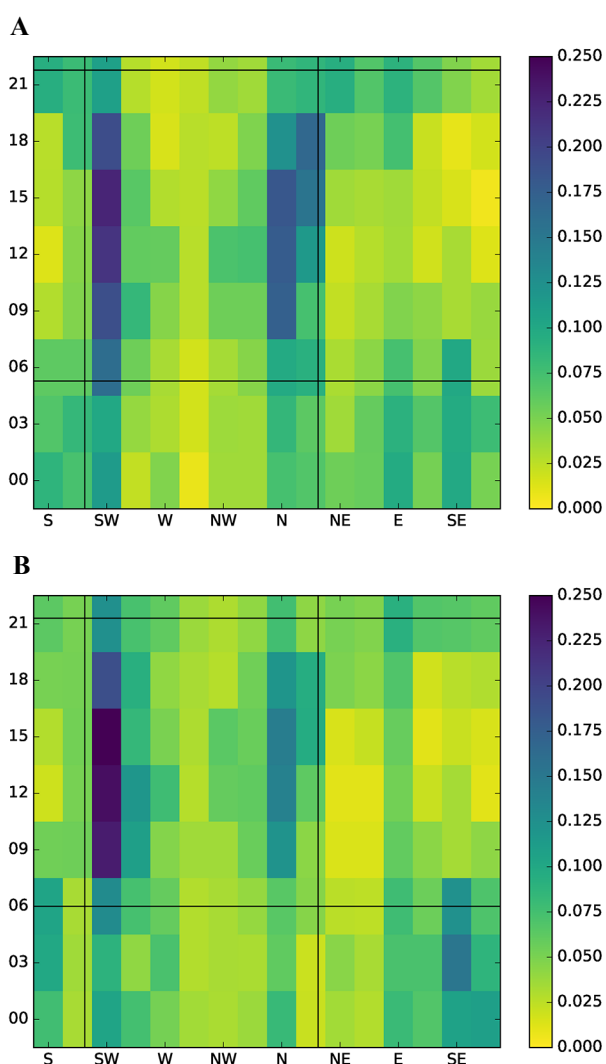
Fig. 1). A similar increase in northern winds during the day can be seen in data from other coastal observation stations (Pāvilosta and Liepāja, figures not shown).

Figure 2 shows no increased frequency of coast perpendicular winds (WNW) that could be interpreted as the classical sea breeze during the day. However, there is an increased frequency of eastern and south-eastern winds before the sunrise that could be interpreted as evidence of land breeze.

The main features of the wind direction distribution for late summer (15 August, Fig. 2B) are similar to those of spring. However, in late summer the southwestern direction is more prevalent than the northern winds and the frequency of southeastern winds before the sunrise (land breeze) is increased.

The wind speed distribution during the cold season (November–February, not illustrated in this paper) shows no pronounced diurnal cycle. The most frequent winds are from the southwestern and southeastern directions.

The results shown in Fig. 2 are similar to those of Soomere & Keevallik (2001). In that paper other stations on the Baltic Sea coast were found to have increased frequency of winds from southwestern and northern directions. The prevalence of southwestern wind in the Baltic Sea region is well known and usually is explained using synoptic-scale processes (Soomere & Keevallik 2001). These processes typically have time scales larger than one day and therefore cannot fully explain the diurnal cycle seen in Fig. 2. In literature (Persson & Kindell 1981; Bergström 1992, both as cited in Soomere & Keevallik 2001) there are reports of a secondary maximum of geostrophic wind from the northeast or east during April–September, but it cannot be easily connected with the maximum from the north and northwest seen in Fig. 2. Shielding from nearby objects is sometimes invoked to explain heterogeneity in the observed wind direction distributions but, to the best of the authors' knowledge, no arguments have been made to explain why the shielding should change throughout the day.

The aim of the rest of this study is to investigate the mechanisms causing the prevalence of northern and northeastern winds seen in Fig. 2.

Event selection for the case study and analysis of the observations

The aim of the case study is to investigate in detail the mechanisms that could lead to the increased frequency of northern winds during daytime in coastal stations. Figure 2a allows us to estimate the number of days in a month when such conditions are present. At 15:00 there is an 18% probability of N wind and 15% probability of NNE wind, which means that there are, on average, 10 days in every month of May in every year that could

Fig. 2. Climatic wind direction distribution, probability (the scale to the right of the figure) of wind from a particular direction (*x*-axis) as a function of time of the day (*y*-axis, local time, UTC + 03 h). Observation data, Ventspils station, corresponding to (**A**) 15 May and (**B**) 15 August (see text for details). Vertical lines indicate the direction of the coastline. Horizontal lines indicate sunrise and sunset hours.

be chosen for further analysis, with a similar number of days in each of the rest of the warm season months.

The years 2013 and 2014 were searched for possible candidate dates for the case study because the recent years have better data availability, e.g., ASCAT data from the METOP-B satellite are available since 2012. The 3rd of May 2013 was chosen because no precipitation was registered in the LEGMC stations and the coast parallel winds on this date could not be explained either by cyclones or atmospheric fronts in the region, and ASCAT data were available over the territory of interest.

The case study is structured as follows. First, the observation data were analysed. Then the ability of the model to represent the observations was examined and next the vertical cross sections of the model results were used to investigate the physical mechanisms that could lead to coast parallel winds.

On 3 May 2013 the synoptic-scale situation was determined by an anticyclone with the centre to the northeast of the region of interest, over Estonia. Most inland stations recorded easterly winds, however, the data from coastal stations on the Kurzeme coast of the Baltic Sea and the satellite data (Fig. 3) show a coast
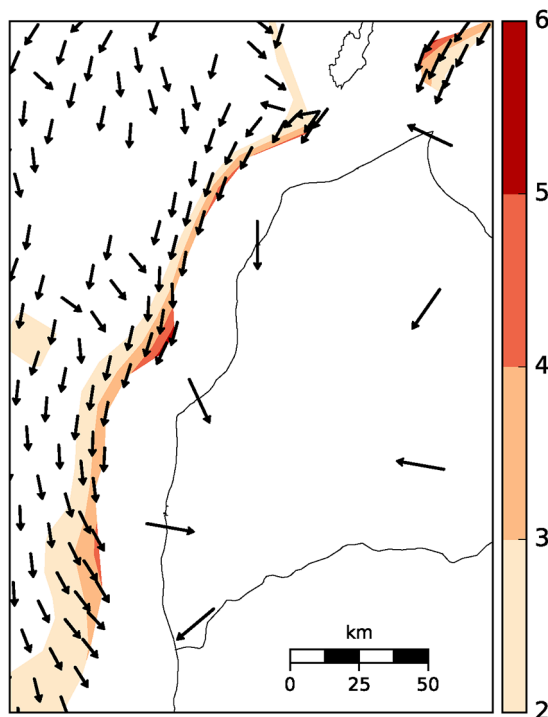
parallel flow oriented from northeast to south, extending approximately 50 km into the Baltic Sea. The time series of 10 min temporal resolution from the observation stations (Fig. 4) show that during the night the wind was blowing offshore, perpendicularly to the coastline (SE, NE). In the morning (09:00) at Ventspils the wind direction rapidly changed into a coast perpendicular onshore flow (NW) for approximately an hour and then switched again to a direction almost parallel to the coast (N). A similar transition took place in the Liepāja station but it happened 3 h later and the wind direction changed smoothly from the coast perpendicular to coast parallel flow.

Numerical modelling and geostrophic wind calculation

A WRF model run was carried out for the selected date. In late morning and early afternoon (12:00–14:00 local time, 9:00–11:00 UTC) model results show a classical, shore perpendicular sea breeze circulation in the northern part of the coastline (Fig. 5A). The calm zone can be observed 30–40 km from the shore. This result is consistent with the observations in the Ventspils station, except for a discrepancy in timing – the model shows the sea breeze circulation starting approximately 2 h later than the observations. A brief period of coast perpendicular wind at 13:00 LT (10:00 UTC) occurs in the Liepāja station, which is never replicated in the model. During that period the southern edge of the sea breeze circulation is located between Ventspils and Pāvilosta.

The model can successfully replicate the shore-aligned flow seen in the ASCAT data, although later in
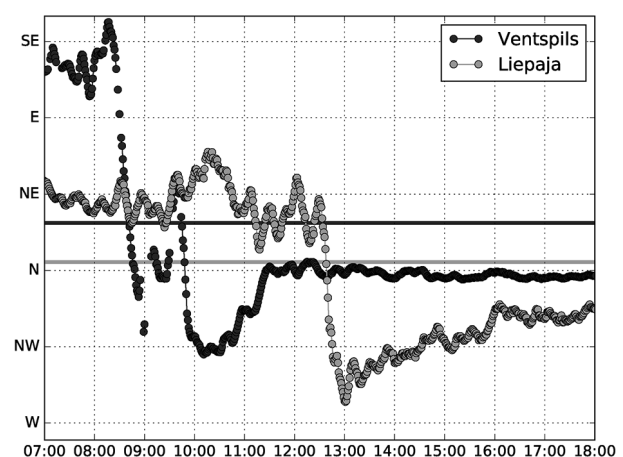

Fig. 3. Wind direction observations on 3 May 2013 at 13:00 (10:00 UTC). ASCAT and observation station data. The wind speed (m/s, scale to the right of the figure) in ASCAT data is indicated by the colours. The size of arrows for the observation stations is exaggerated and the arrows are centred to the station location. ASCAT data copyright (2016) EUMETSAT.

Fig. 4. Wind direction time series in the Ventspils and Liepāja stations for 3 May 2013. LEGMC data, local time (UTC + 03). The orientation of the shorelines is indicated by the horizontal lines.
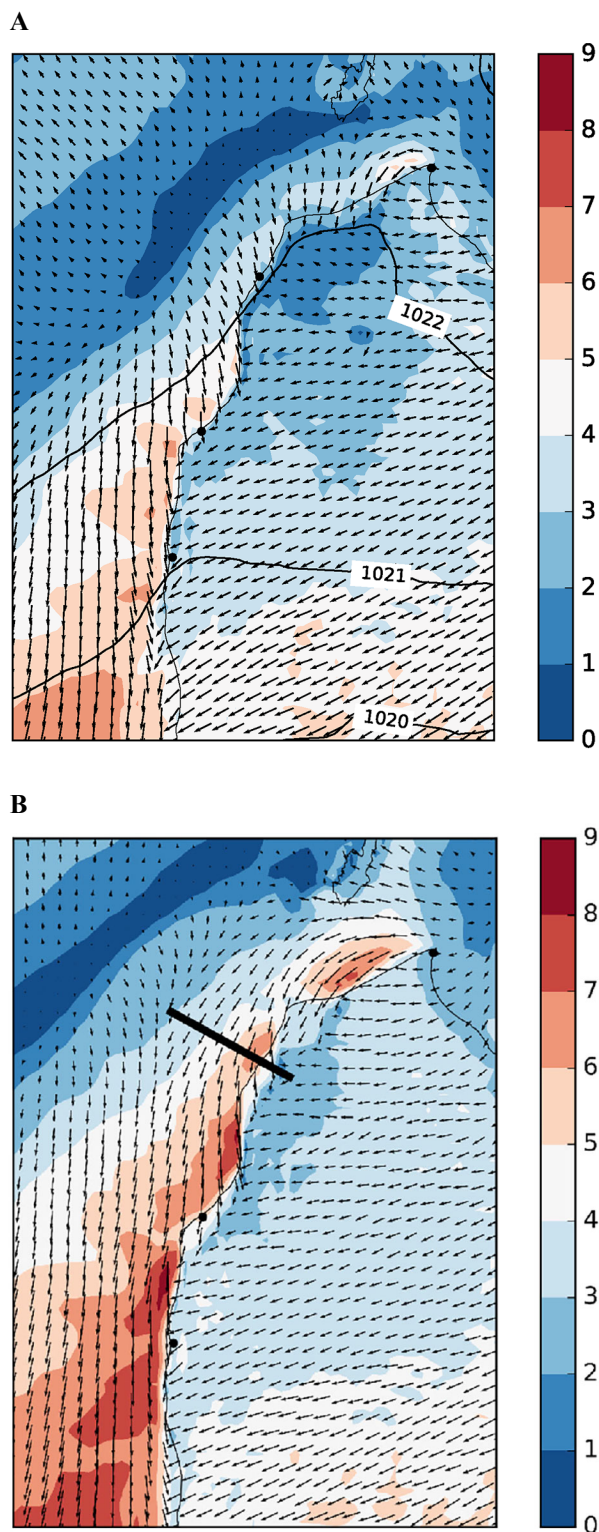
A

B

Fig. 5. The WRF model results, 3 May 2013. Wind speed (m/s, scale to the right of the figure) and direction (arrows) at 10 m height: (**A**) 13:00 (10:00 UTC), (**B**) 16:00 (13:00 UTC). The sea level pressure isobars are shown in (A). The black line in (B) indicates the location of the vertical cross section plotted in Figs 6 and 7.

the day than it is observed (compare Fig. 3 and Fig. 5). The zone of calm associated with the breeze is still present but is located farther from the coast. The wind speed is low to moderate: observation stations have registered wind speeds up to 4–5 m/s and the ASCAT data show wind speed values up to 5 m/s. The model shows values similar to observations for wind speeds onshore (3–5 m/s) and further than 20 km from the shore (6 m/s and lower farther from the coast). Near the shore, where no observations are available, the model predicts higher wind speeds – up to 9 m/s per second.

To summarize, the model replicates the sea breeze circulation in the northern part of the coast and the shore parallel flow seen in observations. The timing, however, is delayed by 2 or 3 h.

We now turn to the analysis of the vertical structure of the wind and temperature fields. The vertical cross section of model results near Ventspils is shown in Fig. 6 (the location of the cross section is depicted in Fig. 5). The wind component perpendicular to the cross section (shore parallel) is plotted to emphasize that this flow is not connected to a coast perpendicular sea breeze circulation. Figure 6 shows that the parallel flow extends vertically up to 500 m and has roughly the same horizontal extent (50 km from the shore) in all levels. The wind speed is maximum and it is located between 50 and 100 m above sea level, near the coastline, therefore this phenomenon can be classified as an LLJ.
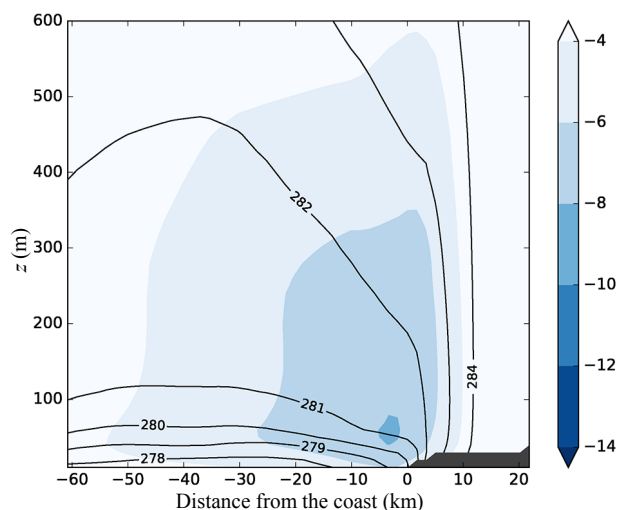

Fig. 6. The WRF model results, 3 May 2013, 16:00 (13:00 UTC). The wind speed component (in m/s, scale to the right of the figure) is perpendicular to the cross section (shown in Fig. 5B) near Ventspils. Negative values represent the wind oriented out of the page, towards the viewer, that corresponds to northeastern wind. Black isolines show potential temperature (in K), z is height above sea level. The positive values of the x-axis are over land, $x = 0$ is the shoreline. The dark grey region on the lower right side shows terrain.
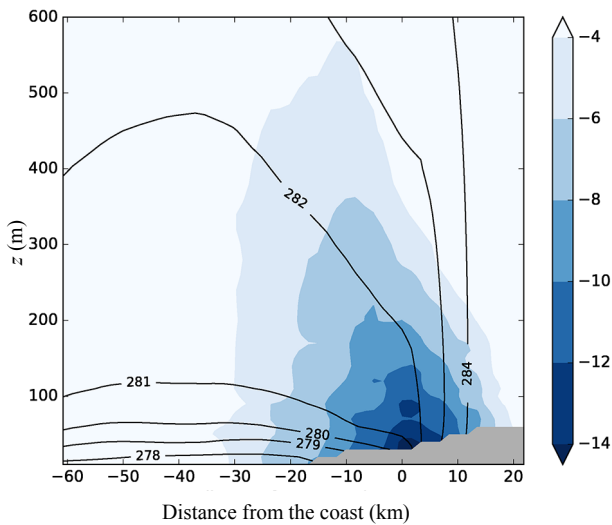
Fig. 7. The WRF model results. The geostrophic wind speed component is perpendicular to the cross section (in m/s, scale to the right of the figure). Black isolines show potential temperature (in K). The location and other parameters are identical to Fig. 6. The light grey zone in the lower right corner indicates the region where data are not available.

Figure 6 shows the wind component perpendicular to the cross section, derived from the horizontal wind speed. Figure 7 is identical to Fig. 6 except that the geostrophic wind component is plotted. The influence of the size of the moving average window used for the pressure field smoothing on the geostrophic wind values was tested. Larger smoothing intervals (21 × 21 km and 27 × 27 km) show similar results and spatial distribution, but the values of wind speed are lower. For instance, if in Fig. 7 the maximum value of the geostrophic wind component exceeds 14 m/s, it would be 11 m/s and 9 m/s for larger smoothing intervals, respectively, but the location of the maxima does not change.

The smoothing procedure also introduces a region where the data are not available because the smoothing window contains a terrain grid point. This region extends horizontally 15 km from the actual terrain.

The comparison between Fig. 6 and Fig. 7 shows that the wind speed values in the LLJ are close to geostrophic and therefore can be analysed in the framework of a CLLJ. More detailed analysis follows in the next section.

DISCUSSION

The thermal wind relationship (Gill 1982) is usually invoked to describe the basic mechanism of a CLLJ:

$$\frac{\partial v_g}{\partial z} = \frac{g}{fT}\frac{\partial T}{\partial x}, \qquad (4)$$

where $g = 9.8$ m/s^2. From Fig. 7 one can estimate that at 100 m height, the temperature T gradient over the coastline $\partial T/\partial x$ is close to 3 K over 30 km, and assuming $T = 280$ K in the denominator, the wind shear explained by the temperature gradient is 3 m/s over 100 m. Figure 7 also shows that the magnitude of the geostrophic wind component on the coastline decreases from 10 m/s at 130 m height to 4 m/s at 330 m height, which means that the shear of the geostrophic wind is also close to 3 m/s over 100 m. Therefore, as seen from Fig. 7, the order of magnitude of the vertical change in geostrophic wind speed is consistent with the temperature gradient over the coastline. Thus the jet could be classified as a CLLJ because its primary mechanism can be explained using coastal baroclinity. However, there are significant differences between this jet and other CLLJs described in the literature. Usually CLLJs have a horizontal scale of 500–1000 km and can exhibit little variation during the diurnal cycle (Muñoz & Garreaud 2005). In our case the horizontal scale is ten times smaller (50–100 km) and the jet exists only during the day. Similarly, the typical values of wind speed are lower when compared to larger CLLJs, where values up to 20 m/s are reported (Muñoz and Garreaud 2005). A feature common with other CLLJs reported in the literature and seen in Fig. 5B is that the wind speed is locally increased downwind of points or capes. This is a well-documented property of a CLLJ and is usually explained using hydraulic theory with the flow being bounded by topography (Burk & Thompson 1996).

The study by Ranjha et al. (2013) using ERA-Interim global reanalysis did not identify the Baltic Sea as a region of significant CLLJ presence. In our opinion, this can be explained by comparing the horizontal extent of the jet seen in Figs 6 and 7 with the horizontal resolution of ERA-Interim that is 80 km, i.e., this jet is too small to be captured in that dataset. Similarly, Tuononen et al. (2015) reported no significant LLJ frequency in the study region during winter months using model data with 30 km resolution. This result is consistent with our observation data which revealed no increase in northern wind frequency seen climatologically during the cold season.

The case study also contained a short episode of sea breeze before the onset of coast parallel flow. If the eastern wind over the land can be assumed to be representative of the background wind direction (note the isobars in Fig. 5A), this event could be classified as a corkscrew sea breeze with the background wind having an alongshore component with the coast on the left

(Miller et al. 2003). Analysing corkscrew sea breezes, Steele et al. (2015) noted the appearance of coast parallel jets and explained them with the Coriolis force acting on shore parallel flows following Hunt et al. (2004). As the sea breeze circulation interacting with background wind has been reported to produce flows that are at small angles with the coastline (Gahmberg et al. 2010), it could be argued that coast parallel flows, such as those seen in Fig. 5B, are a part of the sea breeze circulation. Additional data and discussion that support the argument that the coast perpendicular onshore flow is not the most important feature during the onset of the LLJ are available in the supplementary material at https://doi.org/10.15152/GEO.160.

Cui et al. (1998) showed that for the Californian CLLJ several different directions of background wind can result in a coast parallel LLJ. If their results could be applied here, that could explain the increased frequency of northern winds seen climatologically (Fig. 2).

Climatological analysis (Fig. 2) also revealed an increased frequency of southwestern winds during the day, but the results from this case study cannot be generalized to explain this phenomenon. The direction of a CLLJ is determined by the direction of the temperature gradient – the warmer region should be to the left when looking downwind.

In Soomere & Keevallik (2001), where a similar increased frequency of southern and northern winds was shown for coastal stations in the Baltic Sea, the anisotropy was reported if all the wind speeds were analysed together and for moderate and strong winds, while the distribution of weak winds (less than 6 m/s) was found to be isotropic. In contrast, the wind speeds measured in Ventspils and Liepāja during the case study did not exceed 5 m/s. Soomere & Keevallik (2001) also hypothesized a link with LLJs.

CONCLUSIONS

Long-term wind observations in the coastal stations of the Baltic Proper show an increased frequency of shore parallel winds from the north during daytime in the warm season. A case study was carried out and coast parallel northern winds that were not caused by synoptic-scale phenomena such as cyclones and atmospheric fronts were analysed using meteorological observations, ASCAT data and numerical modelling. The results revealed a short episode of sea breeze that was being replaced by a coast parallel flow over the sea, extending up to 50 km from the shore, with the maximum wind speeds near the coast. The analysis of vertical cross sections of the atmosphere showed that the flow could be classified as an LLJ because the horizontal wind speed

had a maximum below 100 m. The analysis of geostrophic winds showed that the wind speeds in the jet were close to geostrophic and could be described by the thermal wind relationship using the temperature gradient over the coastline. Therefore this event can be classified as a CLLJ.

The case study allows us to explain the increased frequency of northern winds as a mesoscale phenomenon as opposed to an artifact of station siting.

Supplementary online data

Supplementary online data for this article can be found at https://doi.org/10.15152/GEO.160. The document contains Appendix 1, where another case study, similar to the one described in the main text, is carried out for a different date. Appendix 1 contains seven figures and a short description of the main conclusions of the case study.

REFERENCES

Bergström, H. A. 1992. *Climatological Study of Wind Power Potential in the Blekinge Area Using a Meso-γ-scale Higher Order Closure Model*. Wind Energy Report WE 92:01. Department of Meteorology, Uppsala University.

Burk, S. D. & Thompson, W. T. 1996. The summertime low-level jet and marine boundary layer structure along the California coast. *Monthly Weather Review*, **124**, 668–686.

Cui, Z., Tjernström, M. & Grisogono, B. 1998. Idealized simulations of atmospheric coastal flow along the central coast of California. *Journal of Applied Meteorology*, **37**, 1332–1363.

Dee, D. P., Uppala, S. M., Simmons, A. J., Berrisford, P., Poli, P., Kobayashi, S., Andrae, U., Balmaseda, M. A., Balsamo, G., Bauer, P. & Bechtold, P. 2011. The ERA-Interim reanalysis: configuration and performance of the data assimilation system. *Quarterly Journal of the Royal Meteorological Society*, **137**, 553–597.

Dudhia, J. 1989. Numerical study of convection observed during the winter monsoon experiment using a mesoscale

two-dimensional model. *Journal of the Atmospheric Sciences*, **46**, 3077–3107.

Gahmberg, M., Savijärvi, H. & Leskinen, M. 2010. The influence of synoptic scale flow on sea breeze induced surface winds and calm zones. *Tellus A*, **62**, 209–217.

Gemmill, W., Katz, B. & Li, X. 2007. *Daily Real-time Global Sea Surface Temperature – High Resolution Analysis at NOAA/NCEP*. NCEP Off. Note, 260, 39 pp.

Gill, A. E. 1982. *Atmosphere–Ocean Dynamics*. Academic Press, New York, 217 pp.

Floors, R., Peña, A. & Gryning, S. E. 2015. The effect of baroclinicity on the wind in the planetary boundary layer. *Quarterly Journal of the Royal Meteorological Society*, **141**, 619–630.

Holton, J. 2004. *Dynamic Meteorology*. Elsevier Academic Press, 40 pp.

Hong, S. Y., Dudhia, J. & Chen, S. H. 2004. A revised approach to ice microphysical processes for the bulk parameterization of clouds and precipitation. *Monthly Weather Review*, **132**, 103–120.

Hong, S. Y., Noh, Y. & Dudhia, J. 2006. A new vertical diffusion package with an explicit treatment of entrainment processes. *Monthly Weather Review*, **134**, 2318–2341.

Hunt, J. C. R., Orr, A., Rottman, J. W. & Capon, R. 2004. Coriolis effects in mesoscale flows with sharp changes in surface conditions. *Quarterly Journal of the Royal Meteorological Society*, **130**, 2703–2731.

Kain, J. S. 2004. The Kain–Fritsch convective parameterization: an update. *Journal of Applied Meteorology*, **43**, 170–181.

Lebassi, B., Gonzalez, J., Fabris, D., Maurer, E., Miller, N., Milesi, C., Switzer, P. & Bornstein, R. 2009. Observed 1970–2005 cooling of summer daytime temperatures in coastal California. *Journal of Climate*, **22**, 3558–3573.

Lin, Y. L. 2007. *Mesoscale Dynamics*. Cambridge University Press, Cambridge, 433 pp.

Miller, S. T. K., Keim, B. D., Talbot, R. W. & Mao, H. 2003. Sea breeze: structure, forecasting, and impacts. *Reviews of Geophysics*, **41**, 1-1-1-30.

Mlawer, E. J., Taubman, S. J., Brown, P. D., Iacono, M. J. & Clough, S. A. 1997. Radiative transfer for inhomogeneous atmospheres: RRTM, a validated correlated-k model for the longwave. *Journal of Geophysical Research: Atmospheres*, **102**, 16663–16682.

Muñoz, R. C. & Garreaud, R. 2005. Dynamics of the low-level jet off the west coast of subtropical South America. *Monthly Weather Review*, **133**, 3661–3677.

Nunalee, C. G. & Basu, S. 2014. Mesoscale modeling of coastal low-level jets: implications for offshore wind resource estimation. *Wind Energy*, **17**, 1199–1216.

Persson, C. & Kindell, S. 1981. *Nederbördens beroende av den geostrofiska markvinders och den verkliga vindens riktning*. Meddelande No. 8, SMHI, Norrköping.

Ranjha, R., Svensson, G., Tjernström, M. & Semedo, A. 2013. Global distribution and seasonal variability of coastal low-level jets derived from ERA-Interim reanalysis. *Tellus A*, **65**, 20412.

Smedman, A. S., Tjernström, M. & Högström, U. 1993. Analysis of the turbulence structure of a marine low-level jet. *Boundary-Layer Meteorology*, **66**, 105–126.

Soomere, T. & Keevallik, S. 2001. Anisotropy of moderate and strong winds in the Baltic Proper. *Proceedings of the Estonian Academy of Sciences, Engineering*, **7**, 35–49.

Steele, C. J., Dorling, S. R., von Glasow, R. & Bacon, J. 2015. Modelling sea-breeze climatologies and interactions on coasts in the southern North Sea: implications for offshore wind energy. *Quarterly Journal of the Royal Meteorological Society*, **141**, 1821–1835.

Stensrud, D. J. 1996. Importance of low-level jets to climate: a review. *Journal of Climate*, **9**, 1698–1711.

Svensson, N., Bergström, H., Sahlée, E. & Rutgersson, A. 2016. Stable atmospheric conditions over the Baltic Sea: model evaluation and climatology. *Boreal Environment Research*, **21**, 387–404.

Tjernstrom, M. & Grisogono, B. 1996. Thermal mesoscale circulations on the Baltic coast. 1. Numerical case study. *Journal of Geophysical Research – Atmospheres*, **101**, 18979–18997.

Tuononen, M., Sinclair, V. A. & Vihma, T. 2015. A climatology of low-level jets in the mid-latitudes and polar regions of the Northern Hemisphere. *Atmospheric Science Letters*, **16**, 492–499.

Verhoef, A. & Stoffelen, A. 2013. *Validation of ASCAT Coastal Winds*. Technical Report, version 1.5, SAF/OSI/CDOP/KNMI/TEC/RP/176, Sponsored by EUMETSAT.

Aluspinnalähedased lokaliseeritud õhuvoolud Kuramaa rannikuvööndis

Tija Sīle, Juris Seņņikovs ja Uldis Bethers

Kuramaa lääneranniku meteoroloogiajaamades registreeritud tuulesuundade andmestikus 1966–2015 domineerivad suvistel päevadel piki rannajoont puhuvad edela- ja põhjatuuled. Põhjatuulte ebatavaliselt suure osakaalu põhjusi analüüsiti numbriliselt Weather Research and Forecasti mudeliga. Mudeli sisendina kasutati EUMETSAT-i METOP A ja B satelliitidelt pärinevat tuuleinfot. Näidati, et mudel prognoosib kõnesolevatel päevadel piki rannajoont suunatud aluspinnalähedase mõnesaja meetri paksuse õhuvoolu tekkimist. Kõnealune struktuur tekib rannavööndis esinevate õhutemperatuuri ebaühtluste tõttu, järgib ranna asendit ja ulatub rannast 50 km kaugusele. Õhuvool on põhiosas geostroofiline ja selle omadused järgivad temperatuuri muutuste mustrit.